Ammonia Induces a Myostatin-Mediated Atrophy in Mammalian Myotubes, but Induces Hypertrophy in Avian Myotubes

Rachel A. Stern[1]*, Srinivasan Dasarathy[2,3]* and Paul E. Mozdziak[1]

[1] Prestage Department of Poultry Science, North Carolina State University, Raleigh, NC, United States, [2] Department of Pathobiology, Lerner Research Institute, Cleveland Clinic, Cleveland, OH, United States, [3] Department of Gastroenterology, Digestive Disease Institute, Cleveland Clinic, Cleveland, OH, United States

Ammonia, a byproduct of protein catabolism that is generally regarded as toxic, is processed by the liver for excretion. In diseases resulting in hepatic insufficiency, circulating ammonia levels increase dramatically, ensuing secondary disorders. Sarcopenia, or loss of muscle mass, is commonly associated with hyperammonemia. In mammalian models of cirrhosis, increased myostatin is consistent, contributes to muscle autophagy, and reduces satellite cell activation and differentiation, whereas, avian species show a positive myogenic response to ammonia. The objective of the study was to elucidate the effect of ammonia in chicken, mouse, and rat derived myotubes. Primary myoblasts were isolated from the pectoralis major (breast) and biceps femoris (thigh) of embryonic day 17 chicken embryos, and from the hindlimbs of 3-day-old rat pups. C2C12 cells were used for mouse myoblasts. Myotubes were exposed to 10 mM ammonium acetate (AA) or 10 mM sodium acetate (SA) for 24 h to determine myogenic response to ammonia. Relative expression of myostatin mRNA, determined by quantitative real-time PCR, was significantly higher in mammalian myotubes compared to chicken myotubes ($P < 0.001$). Western blot analysis of myostatin protein confirmed a significant increase in ammonia treated rat myotubes, while chicken breast myotubes showed a significant decrease in myostatin ($P < 0.05$). Myotube diameter significantly increased in chicken breast and thigh cultures treated with ammonia, while diameter was significantly reduced in mouse and rat myotubes ($P < 0.05$). Intracellular glutamine is significantly higher in chicken thigh, but not breast, myotubes treated with AA compared to SA treated myotubes ($P < 0.05$). To investigate fiber type differences in ammonia metabolism, Western blot analysis of protein from AA and SA treated myotubes was examined for fast and slow myosin heavy chain isoforms. AA treatment resulted in a higher ratio of fast to slow isoforms of myosin heavy chain in both types of chicken myotubes, while fast isoforms were decreased in AA treated mouse and rat myotubes.

These data demonstrate that chicken myotubes respond positively to ammonia while rodent myotubes respond negatively. Further, there is evidence that ammonia induces a fast fiber type shift in avian muscle, but a slow phenotype shift in mammalian muscle.

INTRODUCTION

In health, or normal physiological conditions, ammonia, which is produced during the breakdown of proteins to amino acids, is predominantly metabolized in the liver and excreted as waste. In patients with hepatic insufficiency, or in diseases, such as cirrhosis, ureagenesis is impaired, resulting in increased circulating ammonia levels, termed hyperammonemia (Rudman et al., 1973; Shangraw and Jahoor, 1999). Excess ammonia, a result of cirrhosis, causes functional impairment of skeletal muscle as it becomes the predominant organ in ammonia detoxification (Olde Damink et al., 2002; Chen and Dunn, 2016). Several studies have shown a direct link between hyperammonemia and sarcopenia, or muscle wasting, in mammalian models of cirrhosis both *in vivo* and *in vitro* (Dasarathy et al., 2004; Qiu et al., 2012, 2013; Tsien et al., 2015; Kumar et al., 2017; Stern et al., 2017). Specifically, ammonia causes skeletal muscle dysfunction and muscle wasting by reducing protein synthesis and cell proliferation, inducing mitochondrial dysfunction, and increasing autophagy (Taylor et al., 2001; Mariño and Kroemer, 2010; Qiu et al., 2012, 2013; Davuluri et al., 2016a,b; Kumar et al., 2017).

Myostatin, a powerful inhibitor of skeletal muscle proliferation and differentiation, has been shown to be consistently upregulated in patients and mammalian models of hyperammonemia, making myostatin regulation a target for combating muscle wasting associated with numerous diseases (McPherron et al., 1997; Taylor et al., 2001; Dasarathy et al., 2004; McFarland et al., 2006; Ju and Chen, 2012; Qiu et al., 2012, 2013; Stern et al., 2017). Strategies for myostatin inhibition are of particular interest in cirrhotic sarcopenia, as it plays a pivotal role in degenerative decline (García et al., 2010). In contrast to mammalian models, previous *in vivo* and *in vitro* studies have shown that avian muscle responds positively to ammonia (Stern et al., 2015, 2017). Specifically, myostatin expression is reduced in avian muscle, when challenged with ammonia, which suggests a positive myogenic environment, prompting questions of physiological differences in ammonia metabolism between avian and mammalian species, including the role of skeletal muscle in ammonia detoxification, skeletal muscle synthesis and storage of glutamine, and potential differences in ammonia metabolism across muscle fiber types.

The objective of the study was to identify differences in ammonia metabolism between species, specifically, alterations in myostatin expression and resulting consequences in myotube characterization in relation to glutamine production, and myofiber phenotype. It is important to understand mechanisms of ammonia metabolism that allow avian muscle to respond positively, which will provide useful insight to therapeutic targets for sarcopenia in mammalian species, and may provide evidence to support the use of ammonia in media supplementation for avian species as a cost-effective additive to improve myofibrillar protein yield.

MATERIALS AND METHODS
Cell Cultures and Treatments

Differentiated myotubes of primary chicken (pectoralis major, biceps femoris), primary rat, and C2C12 cells were used in this study to evaluate species, and fiber type differences in skeletal muscle ammonia metabolism. This study was carried out in accordance with the recommendations of The AVMA Guidelines for the Euthanasia of Animals, American Veterinary Medical Association. The protocol was approved by the North Carolina State University Institutional Animal Care and Use.

Cells

Primary chicken myoblasts were isolated from the pectoralis major (**Breast**), or biceps femoris (**Thigh**) of embryonic day 17 broiler embryos as described (Mozdziak et al., 1996; Stern et al., 2017). Rat myoblasts (**Rat**) were isolated from the hindlimbs of 3-day old CD rat pups (Charles River Labs, Wilmington, MA). Upon arrival, pups were euthanized by decapitation, the hindlimbs were washed with 70% EtOH, and the skin was removed using sterile technique. All muscles of the hindlimbs were surgically removed, avoiding tendons, and placed in a sterile beaker containing Hanks' Balanced Salt Solution (**HBSS,** Sigma Aldrich Life Science, St. Louis, MO) with 1% antibiotic-antimycotic (Sigma Aldrich). The remainder of the cell isolation protocol was performed as described by Stern et al. (2017). Mouse myoblasts (**C2C12**) used in this experiment were passage 5–7 (ATCC, Manassas, VA).

Cell Culture Media

Cells were cultured at 37°C and 5% CO_2 for the duration of the experiments. Chicken and C2C12 myoblasts were cultured in proliferation media consisting of Dulbecco's Modified Eagle's Medium without L-glutamine (**DMEM**, Sigma Aldrich), 15% fetal bovine serum (**FBS**, Genclone, San Diego, CA), 1% Antibiotic Antimycotic Solution (Sigma Aldrich), 1 mM L-glutamine (L-Glutamine, Gibco, Burlington, Ontario, Canada). Proliferation media for rat myoblasts consisted of Hams-F10 media (**F10**, Sigma Aldrich), 20% FBS (Genclone), 1% Antibiotic Antimycotic solution (Sigma Aldrich), and 2.5 ng/mL Recombinant Human FGF basic protein (R&D Systems, Minneapolis, MN). Myoblast differentiation media for all cell types contained DMEM without L-glutamine, 10% horse serum

(Hyclone, Logan, UT), 1% Antibiotic Antimycotic Solution (Sigma Aldrich), 1 mM L-glutamine (Gibco).

Upon fresh isolation, or recovery from frozen storage, cells were plated on 6-well plates (Primaria, Corning, Durham, NC) coated with 0.1% gelatin (Fisher Scientific, Waltham, MA). Primary rat and chicken myoblasts were plated at a density of 175,000 cells/well, while C2C12 cells were plated at 50,000 cells/well; this allowed primary and C2C12 cells to reach 90% confluency at the same rate, 5 days, changing media every 48 h. At 90% confluency, cells were placed in differentiation media, and fed every 24 h for 3 days; this achieved 70–80% myotube fusion in all cell types.

Treatments and Chemicals

After differentiation for 72 h, the myoblast cultures were 70–80% myotubes. Myotubes were then exposed to 10 mM ammonium acetate (**AA**, Sigma Aldrich) or 10 mM sodium acetate (**SA**, Fisher Scientific) in differentiation media for 24 h (37°C, pH 7.4). The treatment of 10 mM ammonium acetate, or 10 mM sodium acetate has been previously determined in separate studies, and has a negligible effect on pH of the treatment media (Qiu et al., 2012; Stern et al., 2017). Treatment media was made fresh, and immediately used, to ensure concentration of ammonium or sodium acetate was accurate. After 24 h of treatment, images were captured using light microscopy (20×, Leica Microsystems Inc., Buffalo Grove, IL) and SPOT camera (SPOT Imaging, Sterling Heights, MI), for visual presentation and myotube diameter measurements prior to harvesting. Treated cells were then removed from the 6-well plates for mRNA extraction, or total protein isolation.

Quantitative Real-Time Polymerase Chain Reaction (qPCR)

After 24 h of 10 mM AA or 10 mM SA treatment, myotubes were removed from the well-using 0.25% trypsin-EDTA (Sigma Aldrich). Cell pellets were washed twice with ice cold PBS and total mRNA was extracted from the cell pellets using the RNeasy Mini Kit (Qiagen, Venlo, Limberg) per the manufacturer's protocol and as previously described in Stern et al. (2017). Total RNA concentration was determined by absorbance at 260 nm, and RNA quality was assessed using agarose gel electrophoresis. Reverse transcription was performed using the High Capacity CDNA Reverse Transcription Kit (Applied Biosystems, Grand Island, NY). qPCR was performed on five samples from each treatment and cell type combination as described by Stern et al. (2015). Six myogenic markers, *myostatin* (*MSTN*), *myogenin* (*MYOG*), *myogenic factor 5* (*MyF5*), *myogenic determination factor 1* (*MyoD*), *myogenic regulatory factor 4* (also known as *MyF6*), and *paired box 7* (*PAX7*) were assessed based on their role in regulating muscle growth and myoblast proliferation and differentiation. β-actin was used as an internal control for normalization of each sample. All experiments were run in triplicate. Fold changes were calculated using the Pfaffl method (Pfaffl, 2001) using SA treated samples as the control. Primer sequences for each gene, species can be found in **Table 1**.

Protein Extraction and Quantitation

Total protein was extracted from the myotube cultures for Western blotting of MSTN protein and fast and slow myosin heavy chain (**MHC**) isoforms, and for quantitation of intracellular glutamine concentration. Briefly, six well plates were washed with ice cold PBS, and placed on ice. While on ice, cold IP lysis buffer (200 µL; ThermoFisher Scientific) was added to each well. Cells were detached from plate by using a cell scraper. The myotube suspensions were passed through a pipet several times, then placed in a bead-beater tube on ice. Each sample was homogenized, without the addition of beads, using a Mini-Beadbeater-1 (Biospec Products, Bartlesville, OK), and placed on ice. Samples were centrifuged at $12,000 \times g$ for 8 min at 4°C to remove undissolved tissue debris. Protein supernatant was removed and placed in a fresh tube for quantitation. The lysate was diluted 1:20 in dH20 and quantified using the Bio-Rad Protein Assay Dye Reagent Concentration (Bio-Rad Laboratories Inc., Richmond, CA). Protein assay standards were also made in 1:20 IP Lysis buffer.

Western Blotting

Total protein samples (40 µg total protein) were boiled 1:1 in Laemmli Buffer (Bio-Rad Laboratories Inc.) and separated by SDS-PAGE using a 10% Mini-PROTEAN TGX stain-free precast gel (Bio-Rad Laboratories Inc.) with a Prometheus Full-Range Protein Ladder (Genesee Scientific, San Diego, CA). Protein was transferred to a PVDF membrane (Merck Millipore, Burlington, MA) and stained with Ponceau-S stain to verify equal protein loading and transfer of samples. Procedures for antibody staining have been previously described in full by Stern et al. (2015). For relative MSTN expression analysis, blots were first stained for MSTN (ab98337 (1:250), Abcam, Cambridge, MA; goat-anti-rabbit, 111-035-003 (1:10,000), Jackson ImmunoResearch Laboratories Inc., Jennersville, PA), stripped and re-probed for β-actin [MA5-15739 (1:1,000), Thermo Scientific, Rockford, IL; donkey-anti-mouse, A16017 (1:10,000), Thermo Scientific]. After blots were stripped, before re-probing, chemiluminescent substrate was applied, and blot was rescanned, to ensure antibody removal. Following rescanning, Ponseau-S stain was applied to the membrane to ensure protein loading remained consistent across the blot.

For relative expression of fast (**F59**) and slow (**S35**) MHC isoforms, blot were first stained with either F59-c (1:300), or S35-s (1:5) primary antibodies, using donkey-anti-mouse (1:10,000) secondary antibody, stripped, then re-probed for the other MHC isoform, stripped again, and finally re-probed for β-actin as previously described (Stern et al., 2017). F59 was deposited to the DSHB by Stockdale, F.E. (DSHB Hybridoma Product F59). S35 was deposited to the DSHB by Stockdale, F.E. (DSHB Hybridoma Product S35). To evaluate differences in MHC expression between cell types, F59 to S35 expression ratio was evaluated for six independent samples treated with sodium acetate from each cell type. MHC evaluation of treatment differences was performed in five independent blots, each with one ammonium acetate-treated and one sodium acetate-treated sample for each cell type, the F59:S35 ratio for ammonium acetate

TABLE 1 | Primer sequences for real-time qPCR.

Species	Primer[a]	Sequence	% Eff	bp size	Spans exon-exon boundary
Avian	MSTN	F 5′-CGGAGAATGCGAATTTGTGTTTC-3′ R 5′-GGGACATCTTGGTGGGTGTG-3′	106	110	NO
Avian	MyoD	F 5′-CGCAGGAGAAACAGCTACGA-3′ R 5′-ATGCTTGAGAGGCAGTCGAG-3′	99	104	YES
Avian	MyF5	F 5′-TGAGGGAACAGGTGGAGAACT-3′ R 5′-ACTCTGCTCCGTCGCGTA-3′	98	185	YES
Avian	MYOG	F 5′-CAGCCTCAACCAGCAGGAG-3′ R 5′-ACTGCTCAGGAGGTGATCTG-3′	93	166	YES
Avian	MyF6	F 5′-AGGCTGGATCAGCAGGACAAAA-3′ R 5′-CGCGGGAATGGTCGGAAG-3′	92	139	YES
Avian	PAX7	F 5′-GAAGGCCTTTGAGAGGACCC-3′ R 5′-GGTTGAATGCTGCGAGTTGG-3′	63	158	YES
Avian	β-ACT	F 5′-GTCCACCTTCCAGCAGATGT-3′ R 5′-TAAAGCCATGCCAATCTCG-3′	85	168	NO
Mouse	MSTN	F 5′-TCACGCTACCACGGAAACAA-3′ R 5′-AGGAGTCTTGACGGGTCTGA-3′	77	166	YES
Mouse	MyoD	F 5′-GCTCTGATGGCATGATGGATT-3′ R 5′-CTATGCTGGACAGGCAGTCG-3′	95	150	YES
Mouse	MyF5	F 5′-AACTATTACAGCCTGCCGGG-3′ R 5′-GCTGGACAAGCAATCCAAGC-3′	89	198	YES
Mouse	MYOG	F 5′-GTGCCCAGTGAATGCAACTC-3′ R 5′-CGAGCAAATGATCTCCTGGGT-3′	96	94	YES
Mouse	MyF6	F 5′-AGAAATTCTTGAGGGTGCGG-3′ R 5′-GCCCCTGGAATGATCCGAAA-3′	108	76	YES
Mouse	PAX7	F 5′-AGTTCGATTAGCCGAGTGCT-3′ R 5′-CATCCAGACGGTTCCCTTTGT-3′	95	142	YES
Mouse	B-ACT	F 5′-AGATCAAGATCATTGCTCCTCC-3′ R 5′-AGCTCAGTAACAGTCCGCCTA-3′	90	170	YES
Rat	MSTN	F 5′-ACAGCAGTGACGGCTCTTTG-3′ R 5′-ATCCACAGCTGGGCCTTTACC-3′	99	175	YES
Rat	MyoD	F 5′-TACGACGCCGCCTACTACAG-3′ R 5′-GCGCTCCACTATGCTGGACA-3′	90	99	YES
Rat	MyF5	F 5′-GCTTTGACAGCATCTACTGCCC-3′ R 5′-GTCCTGAAGAGCCAACTCGGAT-3′	88	137	YES
Rat	MYOG	F 5′-GGGGCAATGCACTGGAGTTTG-3′ R 5′-GTCCACGATGGACGTAAGGGA-3′	97	101	YES
Rat	MyF6	F 5′-ACCGGCTGGATCAGCAAGAG--3′ R 5′-CACCAGGCCCCTGGAATGAT-3′	96	149	YES
Rat	PAX7	F 5′-GTGCCCTCAGTGAGTTCGATT-3′ R 5′-AGTGGGAGGTCGGGTTCTGA-3′	97	191	YES
Rat	B-ACT	F 5′-CCTCTGAACCCTAAGGCCAACC-3′ R 5′-ACACAGCCTGGATGGCTACG-3′	99	94	YES

[a] Primers were designed using Primer-BLAST for MSTN, myostatin; MyoD, myogenic determination factor 1; MyF5, myogenic factor 5; MYOG, myogenin, MyF6, myogenic regulatory factor 4, PAX7, paired box 7; and β-ACT, β-actin.

treatment was normalized to the sodium acetate treatment to correct for blot to blot variations in band intensity.

After secondary incubation and washes, blots were incubated with WesternSure® PREMIUM Chemiluminescent Substrate (LI-COR Biosciences, Lincoln, NE), and images were captured using the C-DiGit Blot Scanner (LI-COR Biosciences). Densitometry was assessed using ImageJ software (imagej.nih.gov/ij/list.html) of five independent blots for MHC relative expression. Relative expression was calculated using β-actin densitometry to normalize each sample. For MSTN relative expression, the mean $\pm$ SE ($n = 4$) was calculated for

each treatment. MHC relative expression is presented as the ratio of fast (F59):slow (S35) mean $\pm$ SE for each treatment.

Intracellular Glutamine Assay

Total protein isolated from myotube cultures treated with 10 mM AA or 10 mM SA were evaluated for glutamine concentration to evaluate intracellular glutamine concentration. Total protein (40 μg) was evaluated of six independent experiments of each treatment and cell type combination using the EnzyChrom™ Glutamine Assay Kit (EGLN-100, BioAssay Systems, Hayward, CA). All samples were run in duplicate, with one sample

blank to account for any changes in intracellular glutamate that could affect the assay results, per the manufacturer's guidelines. Intracellular glutamine was calculated using the provided manufacturer equation, subtracting the sample blank from the average of the duplicate samples. Data is presented as the mean intracellular glutamine concentration of the 6 samples $\pm$ SE.

Myotube Diameter

Myotube diameter was assessed to evaluate differences in physical changes between treatment groups. For each treatment (10 mM AA, 10 mM SA) and cell type (Breast, Thigh, C2C12, Rat) combination, the diameter of 100 myotubes, 10 random myotubes from 10 independent wells was measured using ImageJ software (imagej.nih.gov/ij/list.html). For consistency, diameters were measured at the widest diameter of each linear myotube in the visual field (Stern et al., 2017).

Statistical Analysis

All statistical analysis was performed using JMP 13.2 (SAS Institute Inc., Cary, NC).

Quantitative real-time PCR data is expressed as mean fold-changes of the AA-treated samples compared to the SA control samples, relative to the housekeeping gene, β-actin, $\pm$ SE ($n = 5$ replicates for each). Pairwise comparisons of fold changes of each gene between avian and mammalian species was assessed using Tukey-Kramer HSD test for multiple comparisons ($\alpha = 0.05$). Asterisks represent significant differences in fold change between species (*$P < 0.05$; **$P < 0.01$). Pairwise comparisons between cell types for each gene was performed using the non-parametric Kruskal-Wallis test for multiple comparisons ($\alpha = 0.05$).

MSTN Western blot densitometry is expressed as a mean of bands, relative to the housekeeping protein, β-actin, for each sample $\pm$ SE. Four independent blots were analyzed, and pairwise comparisons were done between treatments for each cell type using a Tukey-Kramer HSD test ($\alpha = 0.05$). Western blot densitometry for MHC isoform expression is expressed as a mean ratio of F59:S35 relative to the housekeeping protein, β-actin, for each sample. Cell type differences in fast to slow MHC ratio (SA treatment only) are expressed as a mean $\pm$ SE of six independent samples of each cell type. Statistical analysis was done using a Tukey-Kramer HSD test ($\alpha = 0.05$). For MHC evaluation of treatment differences five independent blots were assessed, the F59:S35 ratio for ammonium acetate treatment was normalized to the sodium acetate treatment to correct for blot to blot variations in band intensity. Relative densitometry is expressed as the mean F59:S35 ratio $\pm$ SE. Pairwise comparisons between treatments for each cell type was performed using the non-parametric Kruskal-Wallis test. Significance between treatments are represented by asterisks (*$P < 0.05$; **$P < 0.01$).

Intracellular glutamine is presented as the mean $\pm$ SE ($n = 6$). Pairwise comparisons between treatments was done using a Tukey-Kramer HSD ($\alpha = 0.05$). Significant differences between means ($P < 0.05$) are represented by letters.

Myotube diameter was measured for 10 random myotubes from 10 independent wells from each treatment and cell type combination. The mean diameter from each well was calculated and used to compare means between treatments for each cell type ($n = 10$ wells per treatment). Diameter data is presented as the mean $\pm$ SE. Differences between treatments for each cell type was assessed using Tukey-Kramer HSD ($\alpha = 0.05$) and are expressed with letters.
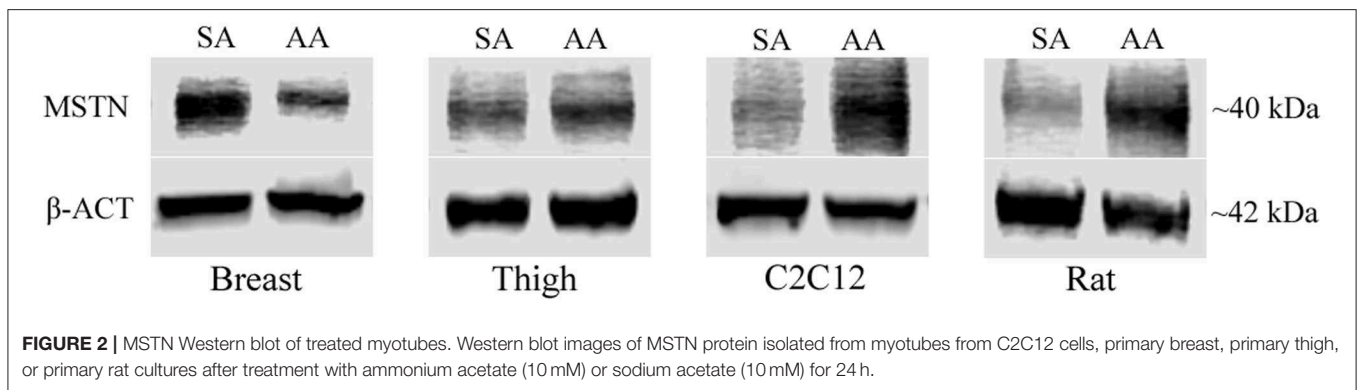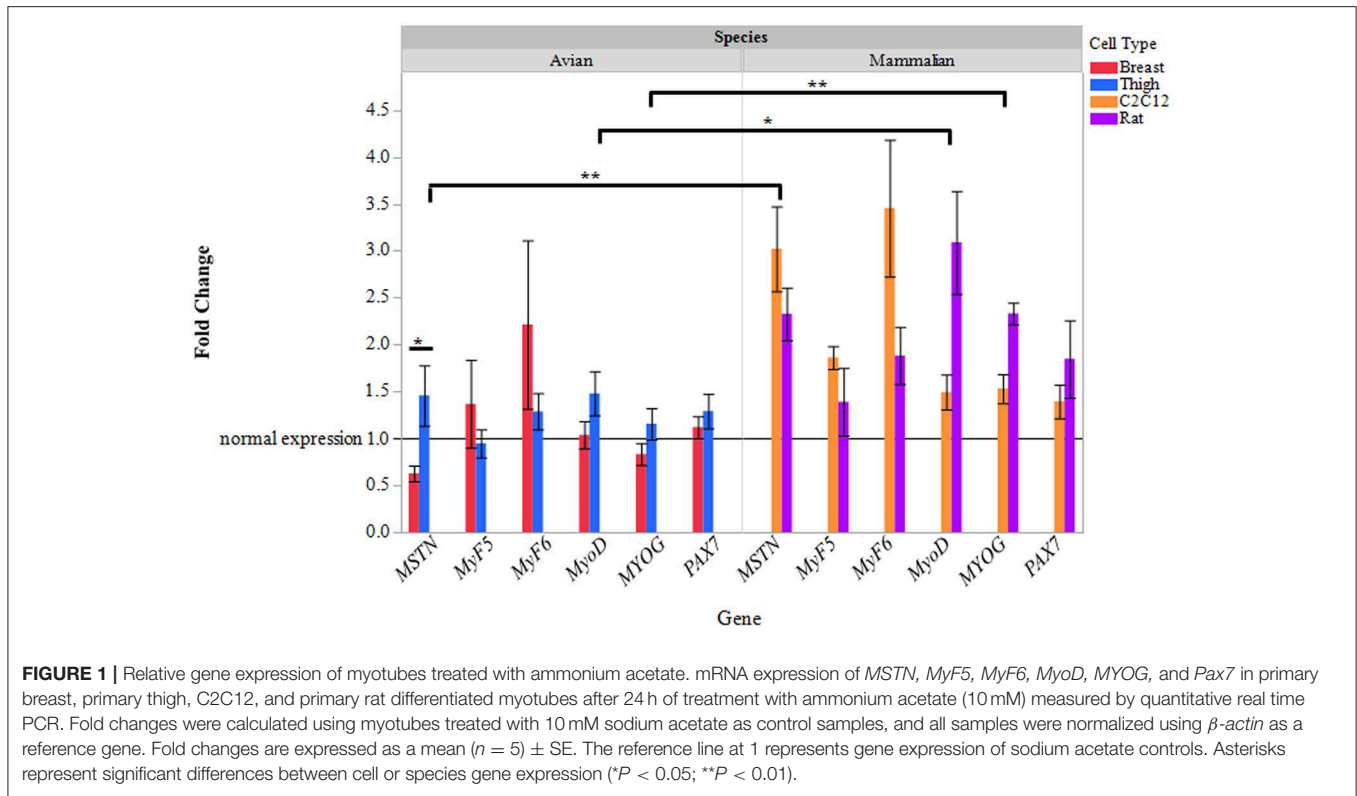
RESULTS

Myogenic Response to Ammonia Differs Between Avian and Mammalian Species

Ammonia Upregulates Myostatin Expression in Mammalian Myotubes

Primary avian (breast, thigh), primary rat, and C2C12 myoblasts were cultured and differentiated (70–80% myotube formation) and treated with ammonium acetate or sodium acetate to evaluate species, and fiber type differences in ammonia metabolism. Quantitative real-time PCR was used to evaluate changes in *MSTN*, and myogenic regulatory factor gene expression in myotubes treated with AA. As displayed in **Figure 1**, relative *MSTN* is significantly higher (2–3-fold) in C2C12 and primary rat myotube cultures, compared to both primary avian myotube cultures ($P < 0.001$). *MyoD* and *MYOG* expression was also increased ($P < 0.05$, and $P < 0.001$, respectively) in mammalian cultures, with rat myotube cultures having higher expression than C2C12. Interestingly, while *MSTN* expression in thigh myotubes treated with ammonium acetate was not changed, relative to sodium acetate treated myotubes, *MSTN* expression was significantly lower in breast myotubes compared to thigh myotubes ($P < 0.05$).

To further evaluate the effect of ammonia on myostatin expression, Western blot analysis of MSTN protein was assessed in avian and mammalian myotubes (**Figure 2**). MSTN protein was significantly higher in Rat myotubes treated with ammonium acetate compared to the sodium acetate-treated controls ($P < 0.05$). MSTN expression in C2C12 myotubes treated with ammonium acetate was not significantly higher compared to treated controls. In contrast, MSTN expression in breast myotubes is significantly lower ($P < 0.05$), and MSTN expression is unchanged in thigh myotubes. **Figure 3** represents the relative densitometry measurements of MSTN bands, compared to each sample β-actin band, for four independent blots.

Myotube Diameter Is Increased in Avian Myotubes Treated With Ammonia

To assess functional effects of altered MSTN expression (**Figures 1–3**), myotube diameter was measured in ammonium and sodium acetate-treated wells. For each cell type, treatment combination 100 myotubes were measured (10 random myotubes from 10 independent wells); mean myotube diameter is presented in **Figure 4**. Correlating with increased MSTN expression, myotube diameter significantly decreased in C2C12 and Rat myotube cultures treated with ammonium acetate, compared to the sodium acetate-treated controls ($P < 0.001$). In contrast, avian myotubes treated with ammonium acetate, both breast and thigh, had a significantly increased mean myotube diameter compared to myotubes in control-treated wells ($P < 0.02$, $P < 0.001$, respectively). Representative

FIGURE 1 | Relative gene expression of myotubes treated with ammonium acetate. mRNA expression of *MSTN, MyF5, MyF6, MyoD, MYOG,* and *Pax7* in primary breast, primary thigh, C2C12, and primary rat differentiated myotubes after 24 h of treatment with ammonium acetate (10 mM) measured by quantitative real time PCR. Fold changes were calculated using myotubes treated with 10 mM sodium acetate as control samples, and all samples were normalized using *β-actin* as a reference gene. Fold changes are expressed as a mean ($n = 5$) ± SE. The reference line at 1 represents gene expression of sodium acetate controls. Asterisks represent significant differences between cell or species gene expression (*$P < 0.05$; **$P < 0.01$).

FIGURE 2 | MSTN Western blot of treated myotubes. Western blot images of MSTN protein isolated from myotubes from C2C12 cells, primary breast, primary thigh, or primary rat cultures after treatment with ammonium acetate (10 mM) or sodium acetate (10 mM) for 24 h.

micropictograph images (40×) of each cell type and treatment are displayed in **Figure 5**.

Ammonia Metabolism Effects Myotube Composition Differently in Avian and Mammalian Species

Intracellular Glutamine Increases in Ammonia-Treated Avian Myotubes

Intracellular glutamine concentration was measured in avian and mammalian myotubes treated with ammonia to determine if applied ammonia had an impact glutamine content. Five independent experiments were evaluated for each treatment and cell type. Intracellular glutamine data for all cell types is reported in **Figure 6**. Thigh myotubes showed a significant increase

in intracellular glutamine after treatment with ammonium acetate, compared to sodium acetate-treated controls ($P < 0.01$). Intracellular glutamine concentration was not significantly higher in Breast myotubes after ammonium acetate treatment ($P = 0.16$). Intracellular glutamine was unchanged in C2C12 and Rat myotubes treated with ammonium acetate ($P > 0.48$, and $P > 0.79$, respectively).

Treatment With Ammonia Causes a Differential Shift in Fiber Type Between Species

Western blot analysis for fast (**F59**) and slow (**S35**) myosin heavy chain isoforms was performed to evaluate fiber type differences in myotubes of different species and tissue origin, in addition to effects of treatment on fiber type.
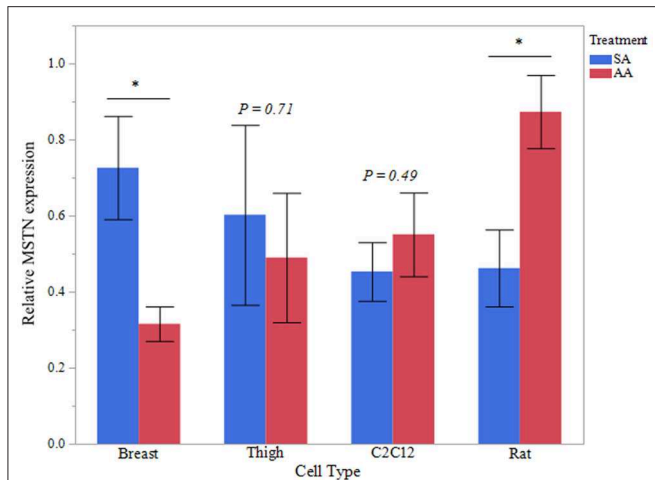
FIGURE 3 | MSTN Western blot densitometry. Relative densitometry of MSTN protein from myotubes from C2C12 cells, primary breast, primary thigh, or primary rat cultures after treatment with ammonium acetate (10 mM) or sodium acetate (10 mM) for 24 h (n = 4 independent samples). MSTN expression is relative to β-actin for each sample. Asterisks represent significant differences between treatments of each cell type (*$P < 0.05$; **$P < 0.01$).
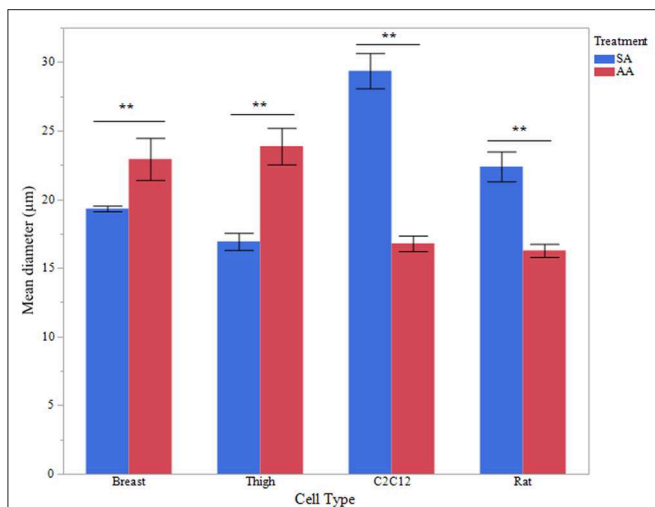

FIGURE 4 | Myotube diameter. Myotube Diameter of primary breast, primary thigh, C2C12, and primary rat myotubes (n = 100 myotubes from 10 independent wells) treated with sodium acetate (10 mM) or ammonium acetate (10 mM) for 24 h. Asterisks represent significant differences between treatments for each cell type (**$P < 0.01$).

FIGURE 5 | Micropictograph myotube images. Representative micropictograph images of myotubes from primary breast, primary thigh, C2C12, and primary rat cultures after treatment with sodium acetate (10 mM) or ammonium acetate (10 mM) for 24 h.

To evaluate fiber type differences between cell origin, sodium acetate-treated myotube cultures were evaluated for fast to slow myosin MHC ratio, mean relative densitometry of F59:S35 ratio is presented in **Figure 7**. There was a significantly increased fast to slow ratio in breast myotubes, compared to Rat and C2C12 myotubes ($P < 0.001$). Thigh fast to slow ratio was also decreased compared to breast myotube cultures ($P < 0.05$).

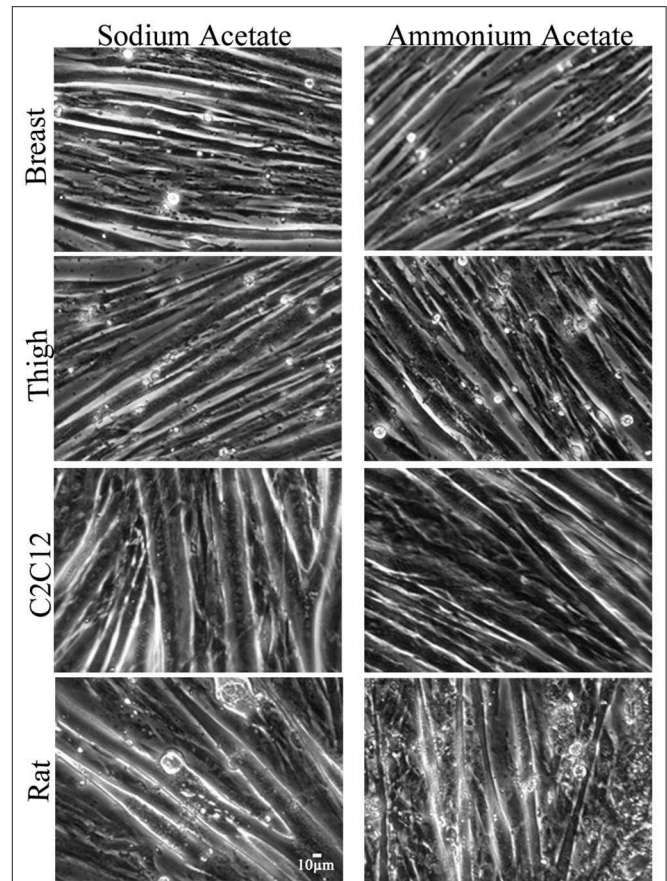To determine if treatment with ammonium acetate influenced fiber type in the myotube cultures, sodium acetate and ammonium acetate-treated samples were evaluated from five independent experiments (**Figure 8**). Treatment with ammonium acetate significantly impacted the myotube phenotype in all cell types ($P < 0.05$), mean relative densitometry of F59:S35 ratio can be seen on **Figure 9**. Both types of avian myotube cultures had a significantly higher fast to slow ratio after treatment with ammonium acetate compared to sodium acetate-treated controls (Breast $P < 0.05$; Thigh $P < 0.01$). Conversely, both C2C12 and Rat myotube cultures had a significantly lower fast to slow ratio after treatment with ammonium acetate ($P < 0.01$).

DISCUSSION

It is well-known that myostatin is a powerful negative regulator of muscle development and post-natal muscle growth (McPherron et al., 1997; Lee and McPherron, 1999; Amthor et al., 2004). It has been well-demonstrated in clinical observation and mammalian models of cirrhosis that myostatin expression is upregulated in response to hyperammonemia, contributing to severe muscle decline (Dasarathy et al., 2004;
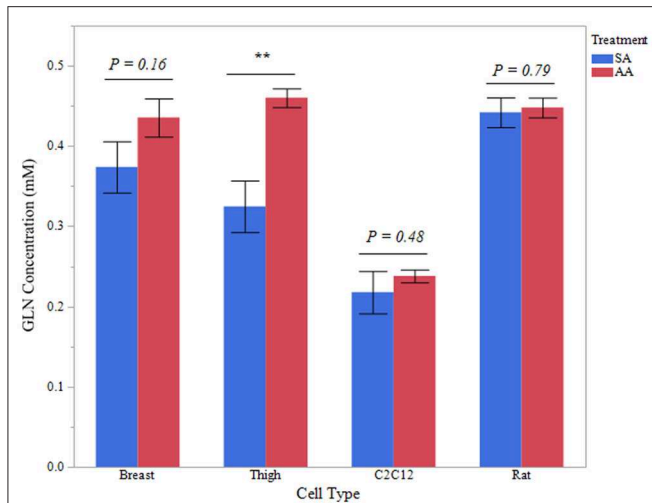
FIGURE 6 | Intracellular glutamine concentration. Glutamine concentration of total protein isolated from primary breast, primary thigh, C2C12, and primary rat myotube cultures treated with sodium acetate (10 mM) or ammonium acetate (10 mM) for 24 h (*n* = 6 independent samples). Asterisk represent significant differences between treatments for each cell type (**$P < 0.01$).
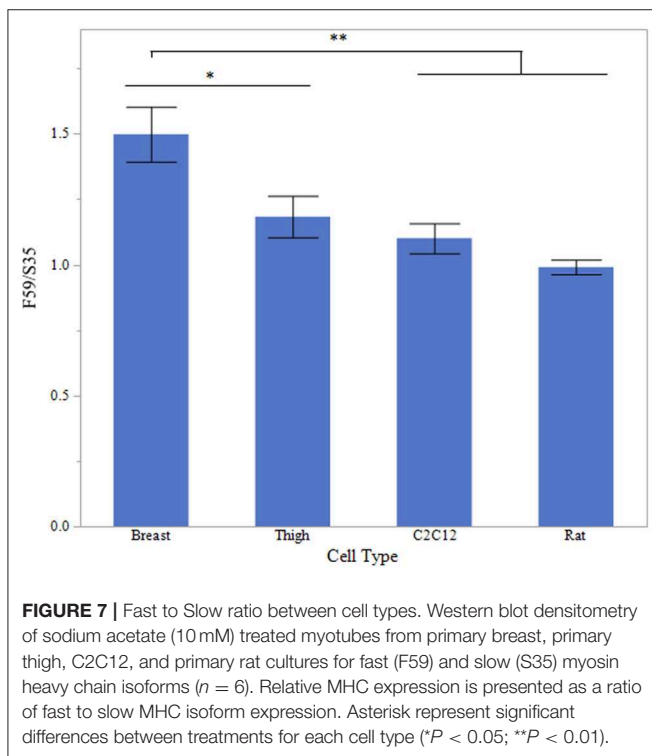

FIGURE 7 | Fast to Slow ratio between cell types. Western blot densitometry of sodium acetate (10 mM) treated myotubes from primary breast, primary thigh, C2C12, and primary rat cultures for fast (F59) and slow (S35) myosin heavy chain isoforms (*n* = 6). Relative MHC expression is presented as a ratio of fast to slow MHC isoform expression. Asterisk represent significant differences between treatments for each cell type (*$P < 0.05$; **$P < 0.01$).

Qiu et al., 2012, 2013; Tsien et al., 2015). Additionally, myostatin has been shown to reduce satellite cell proliferation and differentiation *in vitro* in mammalian and avian species, alike (Taylor et al., 2001; McFarland et al., 2006, 2007). Therefore, regulation of myostatin expression is a targeted therapy for muscle wasting associated with disease and is

important for propagation of myoblasts and muscle tissue in culture.

In contrast to all mammalian models of cirrhosis, which demonstrate that hyperammonemia, or the application of ammonia to myotubes *in vitro*, causes an increase in myostatin expression and decline in myogenic capacity, previous studies have shown that ammonia application to avian muscle results in a decrease in myostatin expression (Dasarathy et al., 2004; Qiu et al., 2012, 2013; Stern et al., 2015, 2017). Though it has been previously demonstrated that C2C12 myotubes and primary breast myotubes have a differential response to ammonia (Stern et al., 2017), comparison of primary avian and primary mammalian myotubes has not previously reported. Additionally, these findings left possible differences in ammonia metabolism between muscle fiber phenotypes in question. Therefore, the central aim of this study was to assess primary avian and primary mammalian myotube cultures, in parallel, for differential responses to applied ammonia between species and myofiber phenotype.

Consistent with previous studies, these studies have shown a transcriptional upregulation of *MSTN* expression in C2C12 and primary rat myotubes after 24 h of ammonia application, that was significantly different than primary avian (Breast and Thigh) myotube expression of *MSTN*. Interestingly, primary breast and primary thigh myotubes also showed a differential response to ammonia application. Expression of *MSTN* was significantly reduced in primary breast myotubes after 24 h of exposure to ammonia, while primary thigh myotubes showed no change in *MSTN* gene expression. Western blot analysis of MSTN protein confirmed qPCR data, showing MSTN reduced in breast myotubes, unchanged in thigh myotubes, and increased in rat myotube cultures after 24 h of exposure to ammonium acetate, compared to sodium acetate-treated controls. In C2C12 ammonium acetate treated myotubes, the increase in MSTN protein was not statistically different from sodium acetate treated myotubes, which may be due to time of treatment incubation. It has been repeatedly shown that exposing C2C12 myotubes to ammonia increases MSTN protein expression, concurrent with an increase in *MSTN* mRNA expression (Qiu et al., 2013; Stern et al., 2017). While it is well-known that increased myostatin expression has a negative effect on myofiber size, both *in vivo* and *in vitro*, myotube diameter of ammonium acetate and sodium acetate-treated myotubes was measured to assess functional impacts of altered MSTN expression. These data demonstrate that increased MSTN expression resulting from applied ammonia in C2C12 and primary rat myotubes, significantly reduces myotube diameter. In contrast, where MSTN expression was reduced or unchanged in avian myotubes treated with ammonium acetate, there was a significant increase in myotube diameter following ammonia treatment.

Glutamine is known to be a major carrier of nitrogen in inter-organ transport, and glutamine synthesis plays a key role in detoxifying ammonia in skeletal muscle, particularly in states of hepatic insufficiency (Wu et al., 1991; Dejong et al., 1994; Olde Damink et al., 2002; He et al., 2010). Additionally, glutamine is an essential amino acid in many cell culture applications, which show that it has a significant impact on optimal cell

proliferation (Yamamoto and Niwa, 1993). Several studies have shown that glutamine synthesis and glutamine utilization differs dramatically between species, and between tissues of the same species (Wu, 1963; Lund and Goldstein, 1969; Meister, 1985). Intracellular glutamine was measured in ammonium acetate and sodium acetate-treated myotubes to determine if glutamine production was initiated in response to applied ammonia. These results demonstrate that intracellular glutamine is increased in avian thigh myotubes when ammonium acetate is applied, suggesting glutamine synthesis may be a method of ammonia utilization in avian muscle. While the assay utilized cannot differentiate between glutamine synthesis and glutamine uptake from the media, sodium acetate-treated myotubes were analyzed to determine basal levels of intracellular glutamine concentration for comparison. Glutamine has been previously shown to prevent hyperexpression of MSTN, which suggests that increased glutamine synthesis in avian myotubes may contribute to an improved response to ammonia, compared to mammalian myotubes (Salehian et al., 2006; Bonetto et al., 2011). Concurrent with a study by Watford and Wu (2005), which states that glutamine synthetase activity is higher in chick leg muscle compared to chick breast muscle, glutamine synthesis in thigh myotube cultures exceeded that of breast myotube cultures, when ammonia was applied to myotube cultures. Altogether, these data suggest that ammonia metabolism may differ between muscle fiber phenotypes within and between species.

To evaluate differences in muscle fiber phenotype between cell origins and between treatments, Western blotting of fast (F59) and slow (S35) myosin heavy chain isoforms was evaluated from total protein isolates. As expected, based on origin of myoblast cells, control-treated primary breast myotube cultures had a significantly higher F59:S35 ratio compared to myotubes cultures originating from thigh muscle. Similarly, breast myotube cultures also had a higher F59:S35 ratio when compared to both primary rat and C2C12 myotube cultures. Interestingly, there was a differential response to applied ammonia between species. Both breast and thigh myotube cultures had a significantly increased F59:S35 ratio in ammonium

acetated-treated myotubes, compared to sodium acetate-treated controls, indicating that ammonia induced a fast fiber type shift in avian myotubes. Increased F59:S35 ratio in breast myotubes can be explained by a significant reduction in myostatin, as it has been shown that myostatin-null rodents have a significant increase in type II, particularly type IIb glycolytic, fibers (Girgenrath et al., 2005; Hennebry et al., 2009). However, myostatin is not significantly reduced in thigh myotube cultures, which like breast myotube cultures, exhibited a fast fiber type shift, and increase in myotube diameter.

Both breast and thigh myotubes demonstrated a significant increase in intracellular glutamine concentration in response to
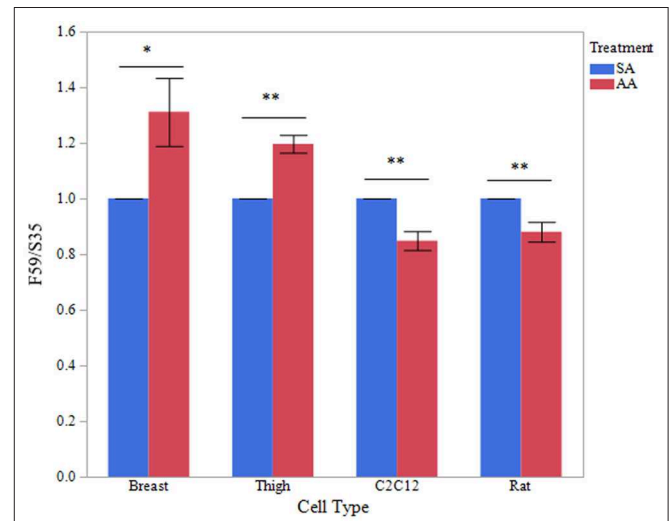

FIGURE 9 | Fast to slow MHC ratio between treatments. Western blot densitometry of sodium acetate (10 mM) or ammonium acetate (10 mM) treated myotubes from primary breast, primary thigh, C2C12, and primary rat cultures for fast (F59) and slow (S35) myosin heavy chain isoforms ($n = 5$). Relative MHC expression is presented as a ratio of fast to slow MHC isoform expression. Asterisk represent significant differences between treatments for each cell type (*$P < 0.05$; **$P < 0.01$).
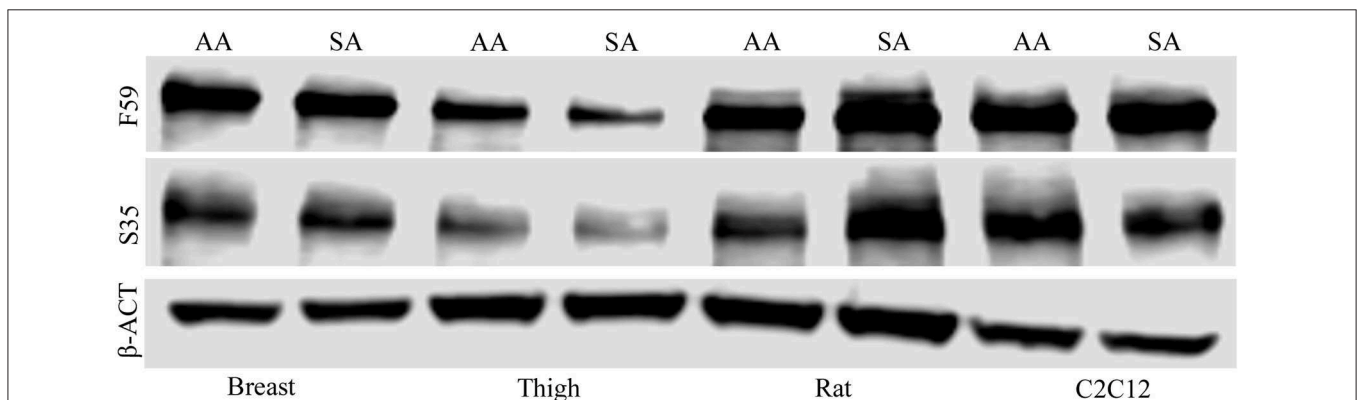

FIGURE 8 | Myosin heavy chain Western blot images. Western blot images of fast (F59) and slow (S35) myosin heavy chain protein isolated from myotubes from C2C12 cells, primary breast, primary thigh, or primary rat cultures after treatment with ammonium acetate (10 mM) or sodium acetate (10 mM) for 24 h. Blots were probed with β-actin to demonstrate equal loading between treatments.

10 mM applied ammonia, therefore, glutamine synthesis is a significant mediator of ammonia metabolism in avian muscle. Interestingly, glutamine has also been reported to activate the Ras/Raf/MEK/ERK pathway, increased ERK phosphorylation (particularly ERK2) has been shown to be increased in fast MHC fiber types in C2C12 cells (Shi et al., 2008; Ayush et al., 2016). Therefore, it is predicted that ammonia is utilized by avian myotubes to produce glutamine, which further supports a fast fiber-type shift in cultured myotubes.

Conversely, C2C12 and primary rat myotube cultures had a significantly decreased F59:S35 ratio when treated with ammonium acetate, suggesting a slow fiber type shift. It is well-understood that in mammalian models of cachexia and sarcopenia that upon activation of the NF-κB pathway, type II, or fast-twitch fibers, are more susceptible to atrophy (Elkina et al., 2011; Schiaffino and Reggiani, 2011; Wang and Pessin, 2013). Relating to cirrhosis, specifically, a previous study has shown that the portacaval anastomosis rat, which is a model for hyperammonemia, has shown that increased circulating ammonia is correlated with an increase in type I, or slow, muscle fibers *in vivo* (Kumar et al., 2017). Altogether, these data suggest that muscle fiber phenotype may play a role in differences in ammonia metabolism and the outcome of hyperammonemia on muscle phenotype between avian and mammalian species.

Alternative media formulations are required to progress the field of cellular agriculture to reduce media cost and move toward serum-free cell growth. For years, ammonia has been regarded as toxic in mammalian cell culture, reducing growth rates, among other issues (Schneider et al., 1996). Conversely, glutamine plays a pivotal role in cell proliferation in cell culture (Yamamoto and Niwa, 1993). The data presented in this study demonstrates that avian myotubes respond positively to applied ammonia and suggests that glutamine production is a method of ammonia utilization. While additional studies would need to be performed to determine the effect of ammonia on cell proliferation, the present study demonstrates that ammonia can be metabolized in avian myotubes. Altogether, these data have shown that ammonia increases protein synthesis, increases myotube growth, and can impact myofiber phenotype in avian myotubes in culture. Incorporating ammonia into avian cell culture media may provide a low-cost alternative to growth and differentiation media in avian cultured meat production in the future.

CONCLUSIONS

These findings provide new evidence that avian muscle responds differently to applied ammonia when compared to mammalian muscle. Myostatin regulation is not only a targeted gene therapy for numerous muscle wasting conditions, but significantly impacts muscle cell proliferation and differentiation *in vitro*. This study shows that reduced MSTN expression in avian myotubes has a significant impact on myotube diameter, supporting the positive response of avian muscle to ammonia. Therefore, identification of mechanisms that allows for a positive response in avian muscle is imperative for developing novel strategies to combat muscle wasting associated with hyperammonemia. In addition to reducing myostatin expression, applied ammonia increased the production of glutamine in avian myotubes. Glutamine is an essential amino acid in cell culture systems, for optimal proliferation of cultured cells, further suggesting that ammonia may be beneficial to avian muscle cells in culture. There is evidence that muscle fiber phenotype plays a role in differences in ammonia metabolism between species, as ammonia induces a fast fiber phenotype shift in avian muscle, but a slow phenotype shift in mammalian myotubes. Understanding the role of the different metabolic profiles of muscle fibers in ammonia utilization may provide further insight in the potential for utilizing ammonia to improve avian muscles cells in culture.

AUTHOR CONTRIBUTIONS

RS performed all experiments, data collection, and analysis for this study and wrote the manuscript. PM contributed to intellectual design and revised the manuscript. SD contributed to the intellectual design of the manuscript.

FUNDING

REFERENCES

Amthor, H., Nicholas, G., McKinnell, I., Kemp, C. F., Sharma, M., Kambadur, R., et al. (2004). Follistatin complexes Myostatin and antagonises Myostatin-mediated inhibition of myogenesis. *Dev. Biol.* 270, 19–30. doi: 10.1016/j.ydbio.2004.01.046

Ayush, O., Jin, Z. W., Kim, H. -K., Shin, Y.-R., Im, S. -Y., and Lee, H. -K. (2016). Glutamine up-regulates MAPK phosphatase-1 induction via activation of Ca2+→ ERK cascade pathway. *Biochem. Biophys. Rep.* 7, 10–19. doi: 10.1016/J.BBREP.2016.05.011

Bonetto, A., Penna, F., Minero, V. G., Reffo, P., Costamagna, D., Bonelli, G., et al. (2011). Glutamine prevents myostatin hyperexpression and protein hypercatabolism induced in C2C12 myotubes by tumor necrosis factor-α. *Amino Acids* 40, 585–594. doi: 10.1007/s00726-010-0683-3

Chen, H. -W., and Dunn, M. A. (2016). Muscle at risk: the multiple impacts of ammonia on sarcopenia and frailty in cirrhosis. *Clin. Transl. Gastroenterol.* 7:e170. doi: 10.1038/ctg.2016.33

Dasarathy, S., Dodig, M., Muc, S. M., Kalhan, S. C., and McCullough, A. J. (2004). Skeletal muscle atrophy is associated with an increased expression of myostatin and impaired satellite cell function in the portacaval anastomosis rat. *Am. J. Physiol. Gastrointest. Liver Physiol.* 287, G1124–G1130. doi: 10.1152/ajpgi.00202.2004

Davuluri, G., Allawy, A., Thapaliya, S., Rennison, J. H., Singh, D., Kumar, A., et al. (2016a). Hyperammonaemia-induced skeletal muscle mitochondrial dysfunction results in cataplerosis and oxidative stress. *J. Physiol.* 594, 7341–7360. doi: 10.1113/JP272796

Davuluri, G., Krokowski, D., Guan, B.-J., Kumar, A., Thapaliya, S., Singh, D., et al. (2016b). Metabolic adaptation of skeletal muscle to hyperammonemia

drives the beneficial effects of l-leucine in cirrhosis. *J. Hepatol.* 65, 929–937. doi: 10.1016/j.jhep.2016.06.004

Dejong, C. H. C., Deutz, N. E. P., and Soeters, P. B. (1994). Muscle ammonia and glutamine exchange during chronic liver insufficiency in the rat. *J. Hepatol.* 21, 299–307. doi: 10.1016/S0168-8278(05)80305-8

Elkina, Y., von Haehling, S., Anker, S. D., and Springer, J. (2011). The role of myostatin in muscle wasting: an overview. *J. Cachexia. Sarcopenia Muscle* 2, 143–151. doi: 10.1007/s13539-011-0035-5

García, P. S., Cabbabe, A., Kambadur, R., Nicholas, G., and Csete, M. (2010). Elevated myostatin levels in patients with liver disease: a potential contributor to skeletal muscle wasting. *Anesth. Analg.* 111, 707–709. doi: 10.1213/ANE.0b013e3181eac1c9

Girgenrath, S., Song, K., and Whittemore, L.-A. (2005). Loss of myostatin expression alters fiber-type distribution and expression of myosin heavy chain isoforms in slow- and fast-type skeletal muscle. *Muscle Nerve* 31, 34–40. doi: 10.1002/mus.20175

He, Y., Hakvoort, T. B. M., Eleonore Köhler, S., Vermeulen, J. L. M., De Waart, D. R., De Theije, C., et al. (2010). Glutamine synthetase in muscle is required for glutamine production during fasting and extrahepatic ammonia detoxification. *J. Biol. Chem.* 285, 9516–9524. doi: 10.1074/jbc.M109.092429

Hennebry, A., Berry, C., Siriett, V., O'Callaghan, P., Chau, L., Watson, T., et al. (2009). Myostatin regulates fiber-type composition of skeletal muscle by regulating MEF2 and MyoD gene expression. *Am. J. Physiol. Physiol.* 296, C525–C534. doi: 10.1152/ajpcell.00259.2007

Ju, C.-R., and Chen, R.-C. (2012). Serum myostatin levels and skeletal muscle wasting in chronic obstructive pulmonary disease. *Respir. Med.* 106, 102–108. doi: 10.1016/j.rmed.2011.07.016

Kumar, A., Davuluri, G., Silva, R. N E, Engelen, M. P. K. J., Ten Have, G. A. M., Prayson, R., et al. (2017). Ammonia lowering reverses sarcopenia of cirrhosis by restoring skeletal muscle proteostasis. *Hepatology* 65, 2045–2058. doi: 10.1002/hep.29107

Lee, S.-J., and McPherron, A. C. (1999). Myostatin and the control of skeletal muscle mass: commentary. *Curr. Opin. Genet. Dev.* 9, 604–607. doi: 10.1016/S0959-437X(99)00004-0

Lund, P., and Goldstein, L. (1969). Glutamine synthetase activity in tissues of lower vertebrates. *Comp. Biochem. Physiol.* 31, 205–210. doi: 10.1016/0010-406X(69)91648-X

Mariño, G., and Kroemer, G. (2010). Ammonia: a diffusible factor released by proliferating cells that induces autophagy. *Sci. Signal.* 3:pe19. doi: 10.1126/scisignal.3124pe19

McFarland, D. C., Velleman, S. G., Pesall, J. E., and Liu, C. (2006). Effect of myostatin on turkey myogenic satellite cells and embryonic myoblasts. *Comp. Biochem. Physiol.* 144, 501–508. doi: 10.1016/j.cbpa.2006.04.020

McFarland, D. C., Velleman, S. G., Pesall, J. E., and Liu, C. (2007). The role of myostatin in chicken (*Gallus domesticus*) myogenic satellite cell proliferation and differentiation. *Gen. Comp. Endocrinol.* 151, 351–357. doi: 10.1016/j.ygcen.2007.02.006

McPherron, A. C., Lawler, A. M., and Lee, S. J. (1997). Regulation of skeletal muscle mass in mice by a new TGF-beta superfamily member. *Nature* 387, 83–90. doi: 10.1038/387083a0

Meister, A. (1985). [27] Glutamine synthetase from mammalian tissues. *Methods Enzymol.* 113, 185–199. doi: 10.1016/S0076-6879(85)13030-2

Mozdziak, P. E., Schultz, E., and Cassens, R. G. (1996). The effect of *in vivo* and *in vitro* irradiation (25 Gy) on the subsequent *in vitro* growth of satellite cells. *Cell Tissue Res.* 283, 203–208.

Olde Damink, S. W. M., Deutz, N. E. P., Dejong, C. H. C., Soeters, P. B., and Jalan, R. (2002). Interorgan ammonia metabolism in liver failure. *Neurochem. Int.* 41, 177–188. doi: 10.1016/S0197-0186(02)00040-2

Pfaffl, M. W. (2001). A new mathematical model for relative quantification in real-time RT-PCR. *Nucleic Acids Res.* 29:e45. doi: 10.1093/nar/29.9.e45

Qiu, J., Thapaliya, S., Runkana, A., Yang, Y., Tsien, C., Mohan, M. L., et al. (2013). Hyperammonemia in cirrhosis induces transcriptional regulation of myostatin by an NF-κB-mediated mechanism. *Proc. Natl. Acad. Sci. U.S.A.* 110, 18162–18167. doi: 10.1073/pnas.1317049110

Qiu, J., Tsien, C., Thapalaya, S., Narayanan, A., Weihl, C. C., Ching, J. K., et al. (2012). Hyperammonemia-mediated autophagy in skeletal muscle contributes to sarcopenia of cirrhosis. *Am. J. Physiol. Endocrinol. Metab.* 303, E983–E993. doi: 10.1152/ajpendo.00183.2012

Rudman, D., DiFulco, T. J., Galambos, J. T., Smith, R. B., Salam, A. A., Warren, W. D., et al. (1973). Maximal rates of excretion and synthesis of urea in normal and cirrhotic subjects. *J. Clin. Invest.* 52, 2241–2249. doi: 10.1172/JCI107410

Salehian, B., Mahabadi, V., Bilas, J., Taylor, W. E., and Ma, K. (2006). The effect of glutamine on prevention of glucocorticoid-induced skeletal muscle atrophy is associated with myostatin suppression. *Metabolism* 55, 1239–1247. doi: 10.1016/j.metabol.2006.05.009

Schiaffino, S., and Reggiani, C. (2011). Fiber types in mammalian skeletal muscles. *Physiol. Rev.* 91, 1447–1531. doi: 10.1152/physrev.00031.2010

Schneider, M., Marison, I. W., and von Stockar, U. (1996). The importance of ammonia in mammalian cell culture. *J. Biotechnol.* 46, 161–185. doi: 10.1016/0168-1656(95)00196-4

Shangraw, R. E., and Jahoor, F. (1999). Effect of liver disease and transplantation on urea synthesis in humans: relationship to acid-base status. *Am. J. Physiol.* 276, G1145–G1152.

Shi, H., Scheffler, J. M., Pleitner, J. M., Zeng, C., Park, S., Hannon, K. M., et al. (2008). Modulation of skeletal muscle fiber type by mitogen-activated protein kinase signaling. *FASEB J.* 22, 2990–3000. doi: 10.1096/fj.07-097600

Stern, R. A., Ashwell, C. M., Dasarathy, S., and Mozdziak, P. E. (2015). The effect of hyperammonemia on myostatin and myogenic regulatory factor gene expression in broiler embryos. *Animal* 9, 992–999. doi: 10.1017/S1751731115000117

Stern, R. A., Dasarathy, S., and Mozdziak, P. E. (2017). Ammonia elicits a different myogenic response in avian and murine myotubes. *Vitr. Cell. Dev. Biol.* 53, 99–110. doi: 10.1007/s11626-016-0088-z

Taylor, W. E., Bhasin, S., Artaza, J., Byhower, F., Azam, M., Willard, D. H., et al. (2001). Myostatin inhibits cell proliferation and protein synthesis in C2C12 muscle cells. *Am. J. Physiol.* 280, E221–E228. doi: 10.1210/jc.82.6.1659

Tsien, C., Davuluri, G., Singh, D., Allawy, A., Ten Have, G. A. M., Thapaliya, S., et al. (2015). Metabolic and molecular responses to leucine-enriched branched chain amino acid supplementation in the skeletal muscle of alcoholic cirrhosis. *Hepatology* 61, 2018–2029. doi: 10.1002/hep.27717

Wang, Y., and Pessin, J. E. (2013). Mechanisms for fiber-type specificity of skeletal muscle atrophy. *Curr. Opin. Clin. Nutr. Metab. Care* 16, 243–250. doi: 10.1097/MCO.0b013e328360272d

Watford, M., and Wu, G. (2005). Glutamine metabolism in uricotelic species: variation in skeletal muscle glutamine synthetase, glutaminase, glutamine levels and rates of protein synthesis. *Comp. Biochem. Physiol. Part B Biochem. Mol. Biol.* 140, 607–614. doi: 10.1016/j.cbpc.2004.12.009

Wu, C. (1963). Glutamine synthetase-I. A comparative study of its distribution in animals and its inhibition by DL-allo-σ-hydroxylysine. *Comp. Biochem. Physiol.* 8, 335–351. doi: 10.1016/0010-406X(63)90169-5

Wu, G. Y., Thompson, J. R., and Baracos, V. E. (1991). Glutamine metabolism in skeletal muscles from the broiler chick (Gallus domesticus) and the laboratory rat (*Rattus norvegicus*). *Biochem. J.* 274, 769–74.

Yamamoto, K., and Niwa, A. (1993). Amino acid and vitamin requirements in mammalian cultured cells. *Amino Acids* 5, 1–16. doi: 10.1007/BF00806187